J Solid State Electrochem (2012) 16:3529–3537
DOI 10.1007/s10008-012-1898-x

ORIGINAL PAPER

Copper nucleation and growth patterns on stainless steel cathode blanks in copper electrorefining

Jari Aromaa · Antti Kekki · Anna Stefanova · Olof Forsén

Received: 19 April 2012 / Revised: 27 September 2012 / Accepted: 29 September 2012 / Published online: 9 October 2012
© Springer-Verlag Berlin Heidelberg 2012

Abstract Surface properties of stainless steel on nucleation and growth of copper under electrorefining conditions were studied using AISI 316L type stainless steel in rotating disc electrodes (RDE), stationary electrodes and Hull cell, and also worn industrial cathode blanks. The aim was to find correlations between surface topography and nucleation and growth using deposition tests, microscopy, and image analysis. Deposition tests were done galvanostatically using synthetic copper electrorefining electrolyte and current density 330 A/m^2 typical in electrorefining. On the as-received stainless steel with 2B finish, nucleation happened at grain boundaries. Wet grinding resulted in deposition on the ridges and valleys of rough surface and ridges of smooth surface. The nucleation density was in the order of 10^6 nuclei/cm^2 in RDE and Hull cell tests, and 10^5 nuclei/cm^2 in stationary electrode tests. Used industrial blanks did not show the same deposition patterns on grain boundaries and scratch marks, and copper deposited on edges of larger damages. The nucleation density on industrial blanks was in the order of 10^3 nuclei/cm^2.

Keywords Stainless steel · Copper · Electrorefining · Nucleation · Surface roughness

Introduction

Electrodeposition of copper is one of the most important deposition processes in industry. Electrodeposition in copper electrorefining and electrowinning is nowadays done on approximately 1 m×1 m stainless steel blanks. Stainless steel cathode blanks are usually made of AISI 316L type steel. The cathode blanks have a typical lifetime over 10 years, but during use the blank surface will collect deposits and become rough due to wear and corrosion. Figure 1 shows examples of unused cathode blank and corroded blank after several years of use. The worn blank shows typical grooves caused by mechanical stripping and corrosion pits. Changing the surface of a substrate even at nanoscale has a strong influence on nucleation and on the initial stages of growth [1]. Therefore, the defects on the surface form nucleation centers and deposits on cathode blank surface can affect the nucleation and growth of copper.

Electrodeposition is a chain of processes beginning with nucleation and followed by bulk diffusion, charge transfer reactions, surface diffusion, and crystallization [2, 3]. Each of these steps is connected with overpotential. Nucleation on a foreign substrate increases with overpotential. The nucleation and deposition of copper on stainless steel depends on the number of active sites that will react at certain overpotential and the overpotential depends on surface film resistance, surface morphology, and additives adsorbed on cathode surface. Stainless steel passive film and additives affect the bond strength between substrate and dissolved copper atoms. If the bond energy between substrate atoms and the metal ions in the electrolyte is high, underpotential deposition can happen and formation of epitaxial layers leading to Frank–van der Merwe layer growth mode or Stranski–Krastanov island growth mode are expected. The three-dimensional nuclei will be formed at surface and film defects [2, 4]. If the bond energy between the substrate atoms and the metal ions in the electrolyte is weak, the discharge of metal ions at surface structures and surface defects will start nucleation. Volmer–Weber island growth mode is now expected [2, 4]. The growth rate of an active grain depends on current density and maximum area that the grain occupies on substrate surface. Growth rate of an active grain is independent of time. The maximum size of grain increases with current density and decreases with nucleation rate [2].

The number of copper clusters on foreign surface has been found to increase with time and overpotential [5] and with

Dedicated to the 75th birthday of Professor Waldfried Plieth

J. Aromaa (✉) · A. Kekki · A. Stefanova · O. Forsén
Department of Materials Science, Aalto University,
PO Box 16200, 00076 Aalto Espoo, Finland
e-mail: Jari.Aromaa@aalto.fi

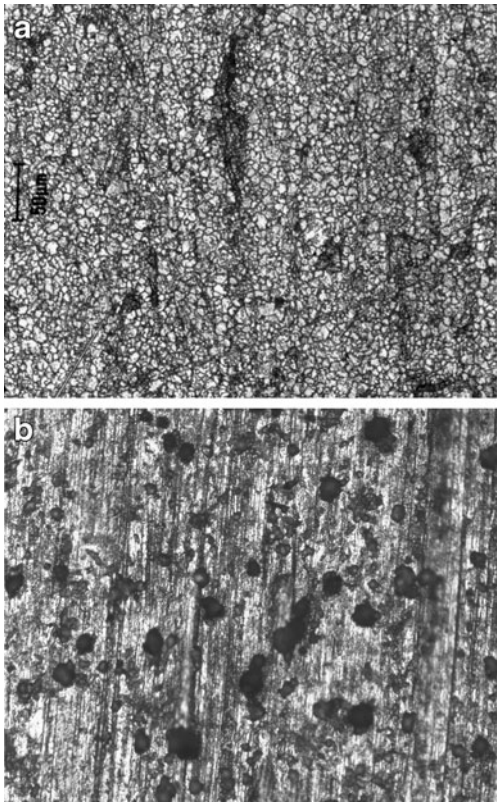

Fig. 1 Unused stainless steel blank with roughness R_a=0.13 μm (**a**) and corroded blank taken from a tankhouse after 6 years with R_a= 1.03 μm (**b**)

increasing current density the clusters become smaller and more copious [6]. Increasing overpotential allows lower energy sites to be available as nucleation centers [7, 8] resulting in a higher number of nuclei [9, 10] or smaller average distance between nuclei [11]. The surface coverage has been found to increase linearly with charge consumed [9].

Surface roughness provides inhomogeneity on the cathode surface and irregularities as nucleation sites. Mechanical treatment of the surface that increases surface roughness increases the nucleation rate constant [12]. The ridges of surface topography will support nucleation at lower overpotential than recesses. On cathode blanks, the number of active sites increases with increasing surface film conductivity [6, 13, 14] and/or surface film porosity [15]. On stainless steel, thicker and more resistive oxide film has been found to limit favorable sites for copper nucleation and result in lower nucleation [16, 17]. Combination of low current density, smooth surface, and presence of chloride ion does not favor formation of a large number of copper nuclei [18].

Experimental

The nucleation tests were done potentiostatically and galvanostatically using rotating disc electrodes (RDE) and galvanostatically using stationary electrodes and Hull cell. The tests were done with EG&G PARC model 273 and AUTOLAB PSTAT 30 potentiostats. The reference electrode was a laboratory-prepared saturated $Cu/CuSO_4$. All potential values in this paper are given vs. $Cu/CuSO_4$.

Different test electrodes were needed because the aim was to find out how the surface morphology and properties affect copper nucleation and growth under conditions that are as close as possible to the industrial practice. The cathode blank material used in copper electrorefining is polished stainless steel. Samples for as-received stainless steel and industrial cathodes were pieces cut from larger sheets and used as stationary electrodes without solution movement. In industrial copper electrorefining, local differences in solution density cause a small upward flow along the cathode surface. Rotating disc electrodes were used to produce a slow electrolyte movement. The rotating disc electrodes cannot produce the same surface features as sheet material samples and the connection between RDE and sheet samples was by wet grinding to produce identical surface roughness. However, as the wet ground sheet material has not the same surface features as the original material, SEM and optical microscopy were used to analyze the preferred areas where copper deposition will start on different samples.

Rotating disc electrode was prepared from AISI 316L 5-mm-diameter steel rod that was cast into epoxy and cut to 1.5-cm pieces. Then 150, 800, and 1200 grit wet grinding papers were used to produce a proper surface roughness. Nucleation tests with stationary electrode and Hull cell were done using 0.5-mm-thick AISI 316L stainless steel with original 2B finish and also prepared by wet grinding using 150 and 1200 grit papers. The 2B finish is produced by cold rolling, annealing, and a further light rolling between highly polished rollers, and it and has an R_a value of between 0.1 and 0.5 μm. Grinding with grit size 150 produces surface roughness R_a=1.0–1.2 μm and polishing with grit size 800 produces bright finish with R_a less than 0.1 μm. For the experiments with real cathode blank samples, 14 industrial cathode blanks from eight companies were received and their properties are given in Table 1. The industrial samples were not treated or cleaned before the experiments.

Tests with RDE were done to see the effect of surface roughness on nucleation type and nucleation sites. The rotating speed 100 rpm was selected based on cathodic polarization curves (0–600 rpm), and it was the highest rotating speed that did not differ from the lower ones. In potentiostatic tests, the sample was polarized to −0.2 V and the resulting current transient was monitored. Galvanostatic tests with RDE were done to verify that active deposition sites were the same when using potentiostatic or galvanostatic control. In these tests, samples were polarized using j=330 A/m^2 and the potential increase (overpotential

Table 1 Coding and properties of industrial blank samples

Sample code	Age (years)	R_a (μm)	Notes
A	12	0.82±0.35	
B1	0	0.34±0.11	New unused cathode
B2	N/A	0.84±0.11	Old cathode from starting sheet production
C	11	0.52±0.12	
D1	3	0.43±0.08	
D2	3	0.44±0.06	
E	11	0.64±0.20	
F1	N/A	1.50±0.45	
F2	N/A	0.96±0.15	
F3	N/A	1.03±0.27	
G1	6	0.63±0.09	
G2	N/A	1.03±0.26	Very much and deep pitting
G3	N/A	0.66±0.13	Deep damages
H	12	1.37±0.21	

decrease) was monitored. Deposition times with RDE were 0.5 s, 2 s, 10 s, and 30 s, and with the three shortest times, separate clusters were seen in SEM analysis. Galvanostatic tests with stationary samples, Hull cell, and industrial blank samples were then done to see the effect of surface properties on nucleation sites and nucleation and growth rate. With stationary samples and industrial samples, the current density was 330 A/m^2 and the Hull cell tests were analyzed using the j=330 A/m^2 range. Also, in these tests the potential change was monitored. For the stationary samples and Hull cell tests, deposition times were from 10 to 300 s. Shorter times did not produce enough copper for image analysis and longer times did not allow separation of copper and stainless steel in the image analysis anymore. Deposition times with industrial blanks were selected based on the tests with stationary samples and they were from 10 to 60 s.

From the stationary AISI 316L 2B samples, Hull cell tests and industrial blanks, the number of copper clusters, their size and distribution, and copper coverage on steel were analyzed using optical microscope images and ImageJ and Adobe Photoshop software. With image analysis software, ImageJ color images were converted first to 8-bit black and white pictures, and contrast was increased. This procedure produced images where only the dark copper areas remained visible. The software calculated the number of independent black (copper) areas, their size, and the area coverage. With Adobe Photoshop software, it was not necessary to convert first to black and white image. A macro was written to increase the contrast of copper particles and the software then selected areas based on the color and calculated number of particles and copper coverage.

The industrial copper electrorefining electrolyte consists mainly of sulfuric acid and copper ions with varying amounts of nickel and arsenic ions. The minor elements include other metal ions, chloride ions, and organic additives. The electrolyte in refineries using permanent cathodes contains 42–49 g/l Cu, 160–190 g/l free H_2SO_4, and 36–56 ppm Cl^-. The temperature range is 62–68 °C. The current density is 260–340 A/m^2 [19]. In this work, the electrolyte contained 180 g/l H_2SO_4, 45 g/l Cu^{2+}, 15 g/l Ni^{2+}, and 10 g/l As, and the same electrolyte was used in all tests. Chloride concentration was adjusted with 1 % HCl solution to 10 or 100 mg/l. Fresh solutions containing 2 mg/l gelatine and 2 mg/l thiourea were made every day to avoid decomposition of the surface active additives.

Results

The first test series was done using AISI 316L type stainless steel to estimate the effect of surface morphology on nucleation sites. These tests were done using RDE and sheet electrodes for stationary electrodes and Hull cell cathodes. The second test series was done using cathode blank samples from several companies. The purpose of the second test series was to study nucleation and growth on corroded and unclean surfaces typical for industrial production. Tests with industrial blank samples were done using stationary electrodes.

Tests with stainless steel

Figure 2 shows potentiostatic transients measured with rotating disc electrode for 150 grit, 800 grit, and 1200 grit finishes. During the first 10 s, the sample has almost reached a steady state with current density of approximately 400 A/m^2. The steady-state current densities were more than one order of magnitude higher than those measured

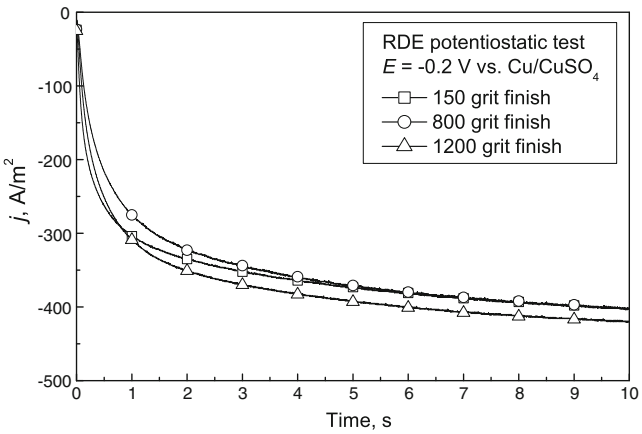

Fig. 2 Potentiostatic test with rotating disc electrode. The current increases most rapidly on 1200 grit sample

with glassy carbon electrodes in [20]. Plotting the transients of Fig. 2 as j vs. $t^{3/2}$, the 800 grit and 1200 grit finishes showed a short initiation period followed by linear dependence indicating progressive nucleation controlled either by hemispherical diffusion or ohmic effects [4]. However, the linear period was very short.

Short galvanostatic pulses were also done with rotating disc electrode (Fig. 3). In galvanostatic tests, the samples reached a steady state very rapidly. The final potentials were −50… −70 mV vs. Cu/$CuSO_4$. The 150 grit sample had the lowest potential (highest overpotential) and 800 grit and 1200 grit samples were quite identical. Under galvanostatic polarization, the overpotential η decreased with time as more and more copper deposited on the surface. The potential change rate was estimated using absolute potential values. Using the data in Fig. 3, the calculated log|E| vs. log(t) slopes were −0.21± 0.01 for 150 grit sample, −0.24±0.01 for 800 grit sample, and −0.25±0.01 for 1200 grit sample. The smoother the surface, the faster is the potential increase (overpotential decrease) indicating faster coverage by copper.

Figures 4 and 5 show scanning electron microscopy (SEM) images of the potentiostatically, at −0.2 V, deposited copper clusters on the RDE samples. The copper clusters follow the scratch lines. Figure 4 shows a sample treated with roughest 150 grit sandpaper, and copper has electrodeposited on both profile peaks and valleys. On the smoother 800 grit and 1200 grit surfaces, the deposition pattern prefers profile peaks (Fig. 5). On the RDE electrode with 150 grit surface finish, the nucleation density was 8.2×10^6 clusters/cm^2 after 2 s and 8.0×10^6 clusters/cm^2 after 10 s, with 800 grit surface finish 7.6×10^6clusters/cm^2 after 2 s and 3.6×10^6clusters/cm^2 after 10 s, and with 1200 grit surface finish 6.6×10^6clusters/cm^2 after 2 s and 6.8×10^6 clusters/cm^2 after 10 s. The size of the clusters was 0.5–1 μm after 2 s and 1–2 μm after 10 s for all RDE samples. Figures 4 and 5 show that deposition on 150 grit polished

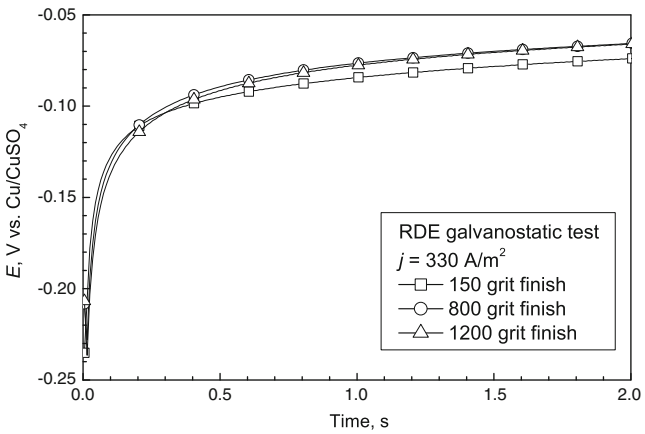

Fig. 3 Potential change in galvanostatic tests with rotating disc electrode

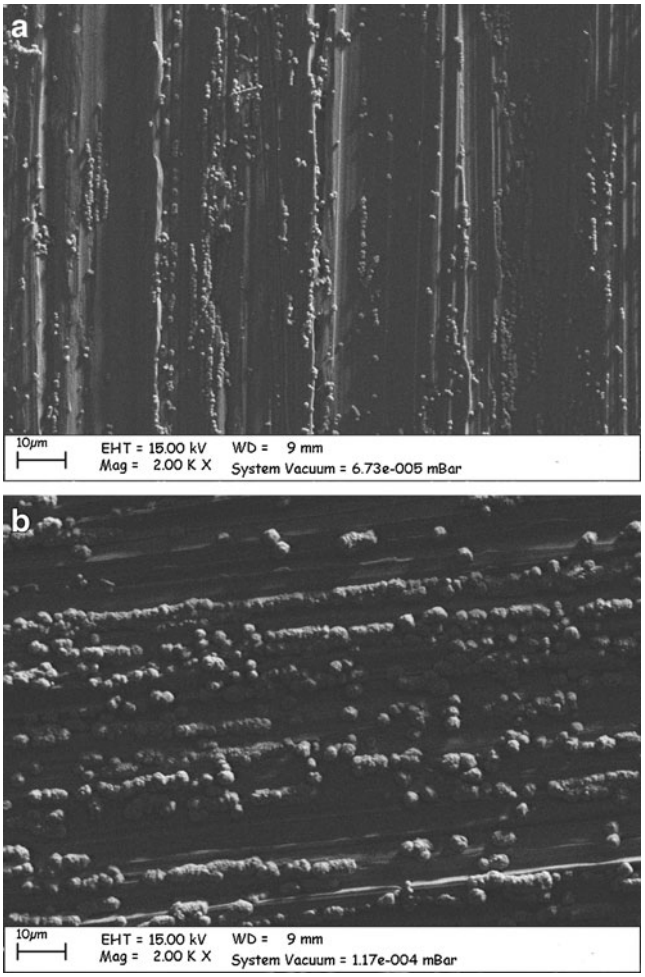

Fig. 4 RDE test with 150 grit water ground paper treatment, deposition times 2 s (**a**) and 10 s (**b**), magnification ×2,000

sample covers the surface slower than deposition on smoother 1200 grit polished sample. The trend is the same that was found for galvanostatically deposited RDE samples when comparing their potential change rates.

Both potentiostatic and galvanostatic RDE tests have shown that copper deposits preferentially on the scratch marks. Nucleation and growth patterns were then measured with galvanostatic tests using stationary electrodes. The deposition times were 10 s, 60 s, 120 s, and 300 s. The copper growth was analyzed using optical micrographs and ImageJ software. Figure 6 shows deposits on 150 grit finish surface. The copper deposition pattern followed again the surface morphology. The analysis of cluster density was possible only with 10 s deposition time and it was 3.5–7.0×10^5clusters/cm^2. The average diameter of clusters after 10 s was 2–4 μm and after 60 s 10–20 μm.

The potential increase in stationary electrode tests was slower than in the RDE tests. A steady potential was achieved usually after 60–120 s. The potential change rates calculated as log|E| vs. log(t) slopes were −0.05…−0.07.

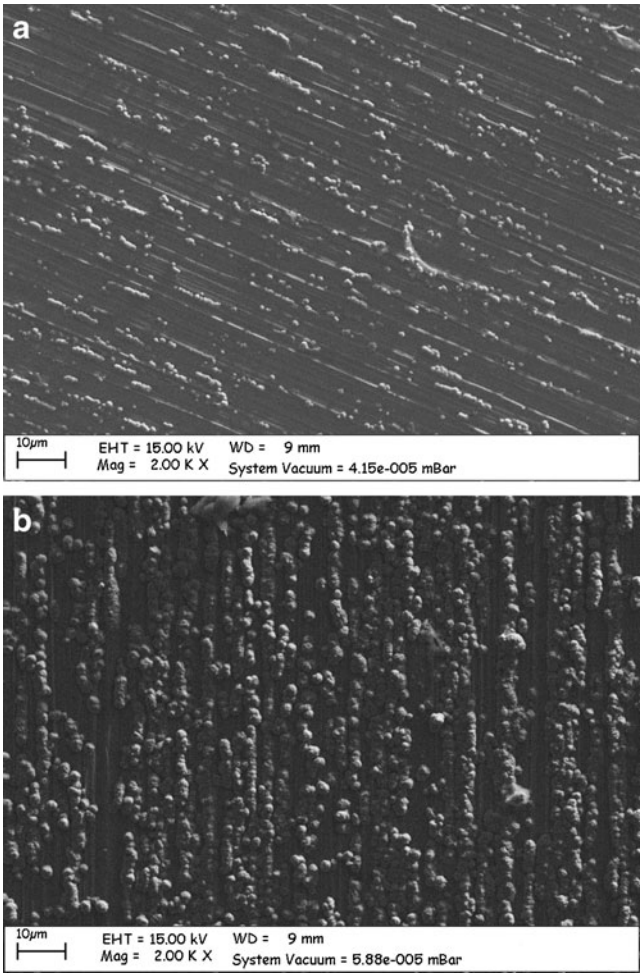

Fig. 5 RDE test with 1200 grit water ground paper treatment, deposition times 2 s (**a**) and 10 s (**b**), magnification ×2,000

The surface coverage increased first rapidly but then slowed down. Even after 300 s deposition time, the surface was not wholly covered as in the beginning deposition is preferred on the peaks and valleys over the even surface. As copper area grows following the pattern of scratch marks, the overpotential decreases with time and at the later stages it will not be high enough to initiate nucleation and growth between the areas of growing copper. Using the copper area percentage from the four different deposition times, it was estimated that the copper area growth followed a power law (Fig. 7). Equation (1) shows copper growth as a function of time for 150 grit sample, Eq. (2) for 1200 grit sample, and Eq. (3) for original 2B surface.

$$\text{Log (area) } [\%] = (1.20 \pm 0.01) + (0.30 \pm 0.01) \cdot \log(t) \text{ [s]} \quad (1)$$

$$\text{Log (area) } [\%] = (0.58 \pm 0.08) + (0.51 \pm 0.04) \cdot \log(t) \text{ [s]} \quad (2)$$

$$\text{Log (area) } [\%] = (0.51 \pm 0.15) + (0.45 \pm 0.08) \cdot \log(t) \text{ [s]} \quad (3)$$

On rough 150 grit surface, initial coverage was larger than on smoother 1200 grit surface or original 2B surface, but the coverage increased slower than on the smoother surfaces. On the original 2B surface, the initial coverage

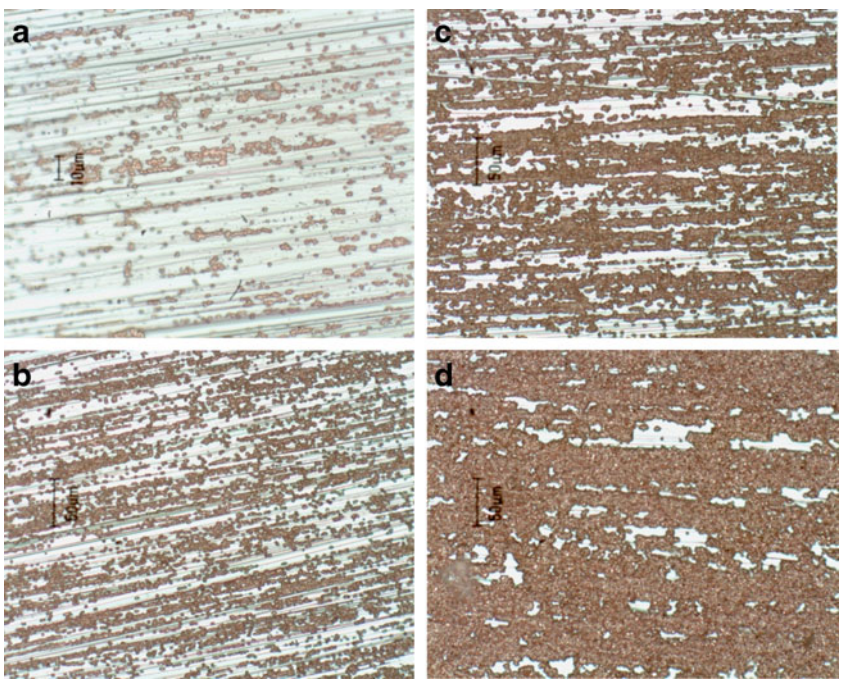

Fig. 6 Growth of copper deposited using j=330 A/m^2 on samples polished with 150 grit, **a** 10 s, **b** 60 s, **c** 120 s, and **d** 300 s deposition time

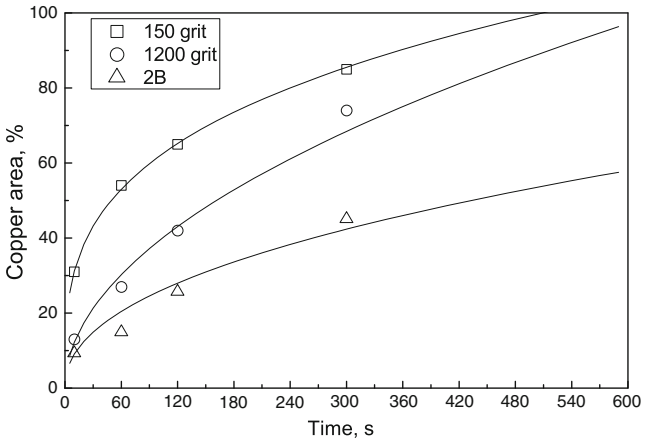

Fig. 7 Copper coverage on stationary 2B, 150 grit, and 1200 grit samples

was smaller than on the abraded surfaces and the growth rate was also slowest.

Galvanostatic transients were measured in the Hull cell for untreated 2B finish, 150 grit, and 800 grit polished samples. The measured potential value increased (overpotential decreased) with time as with the RDE and stationary electrodes. The overpotential of as-received 2B sample was higher than that of the treated samples. The potential difference between 150 grit and 800 grit surfaces was not large, but the overpotential was slightly lower for rougher 150 grit sample. Also in Hull cell tests at j=330 A/m^2 after deposition times of 30 s, the deposits followed the scratches on the surface and copper islands started to deposit from some of the grain boundaries. At longer times, the deposition pattern was clearly growth of separate islands. Figure 8 shows SEM images of Hull cell cathodes taken at current density j= 330 A/m^2 area. On the original 2B surface, all copper clusters are located on grain boundaries. The estimated number of clusters on 2B sample in Fig. 8 is 2×10^5 clusters/cm^2 and the cluster size was 0.5–1 μm. On the 150 grit treated surface, there were many very small nucleation sites compared to 2B surface. The density was 4.2×10^6 clusters/cm^2, also over ten times larger than on 2B surface. The size of clusters was slightly smaller than those in 2B sample and the smallest clusters were 0.2–0.5 μm. Even the largest clusters were less than 1 μm. On the 150 grit treated sample, copper was mostly deposited around the scratches, both bottom and edges, and at some of the grain boundaries of the steel.

Tests with industrial blanks

The second test series was done for used industrial blanks by galvanostatic deposition in a three-electrode cell. The sample overpotential was measured and copper deposits were counted using image analysis. Figure 9 shows

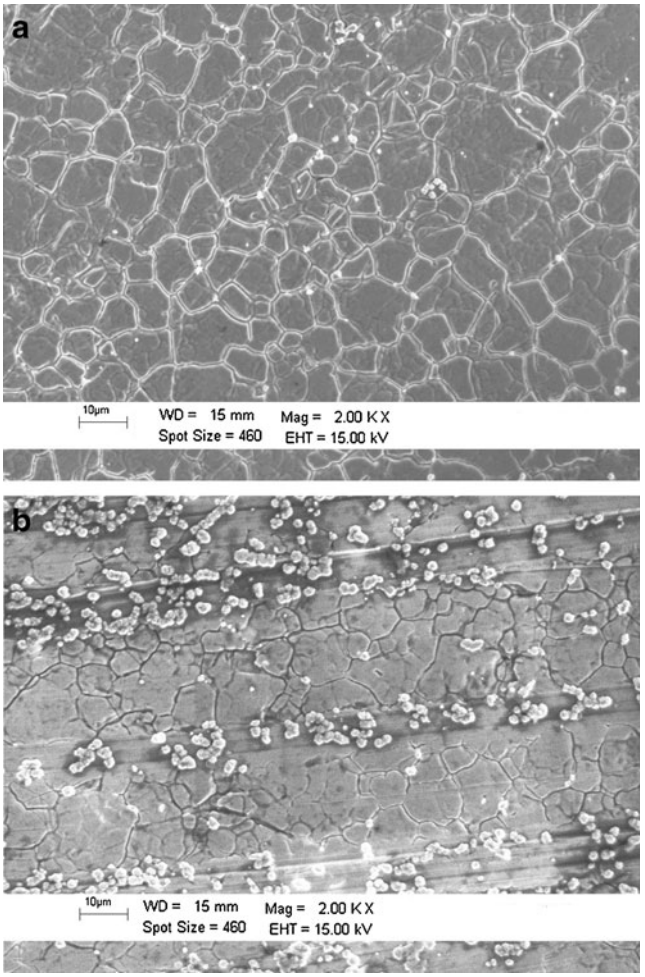

Fig. 8 SEM images from Hull cell cathodes at j=330 A/m^2 after 10 s deposition time, original 2B surface (**a**) and 150 grit treated surface (**b**), magnification ×2,000

examples of the overpotential with time. Usually, the overpotential decreased continuously. In some samples, the overpotential increased first and after a period of less than second it started to decrease, like for industrial sample B2 in Fig. 9. This has been interpreted that progressive nucleation occurred first and after reaching the maximum overpotential current was consumed in growth of copper crystals [1, 21]. As the time to reach maximum overpotential decreases with applied current density and absence of surface films [21], it is very likely that in most of the tests the change from nucleation to growth period happened in less than 0.1 s and it was not recorded. The overpotential changes could not be correlated with measured surface properties or blank age. The overpotentials of industrial blanks were higher than those of stainless steel and the final potentials varied strongly from −0.13 to −0.30 V. This indicates that the industrial blanks have more resistive surface film that includes deposits from the electrolyte and not only the typical passive film of stainless steel.

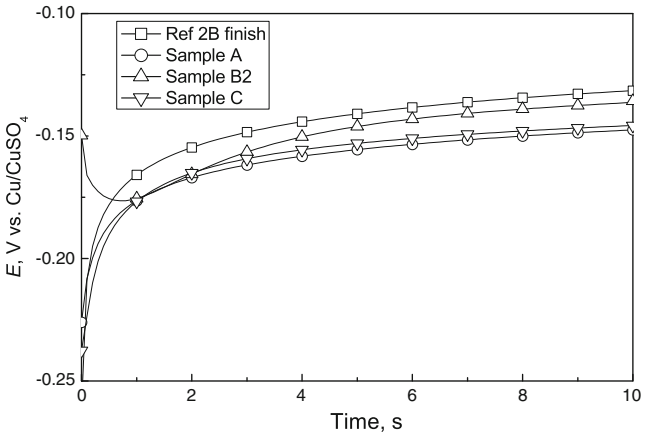

Fig. 9 Potential change in galvanostatic tests with industrial cathodes

Figure 10 shows examples of copper growth patterns on industrial cathode blanks. The images indicate that nucleation and growth on inhomogeneous surfaces depends very strongly on the surface features. The small recesses like grain boundaries and scratch marks and large damages like corrosion pits do not behave identically. Copper growth prefers edges of larger damages over shallow scratch marks, grain boundaries, or plane surface. This can result from secondary current distribution as local current density concentrates on sharp edges.

The changes in copper cluster density and copper area with time obtained from image analysis were combined with the surface roughness data shown in Table 1. The cluster densities and copper areas as function of surface roughness are shown in Figs. 11 and 12. The cluster density at different times depends on the number of initial nuclei and how they grow together with time. For most of the samples, the cluster density decreased from 10 s to 30 s deposition time and then increased from 30 s to 60 s. The cluster density decreased only slightly with increasing surface roughness for 10 s and 30 s deposition times, but for 60 s deposition time this trend was clear (Fig. 11). The copper area increased with time and usually there was a strong increase in the coverage between 30 s and 60 s. The coverage was independent of surface roughness for 10 s and 30 s deposition times but decreased with increasing surface roughness for 60 s deposition time (Fig. 12). The decrease in cluster density and surface coverage with increasing surface roughness supports the growth patterns shown in Fig. 10 that on a rough stainless steel blank surface, copper nucleation and growth is dominated by the large damages with sharp edges.

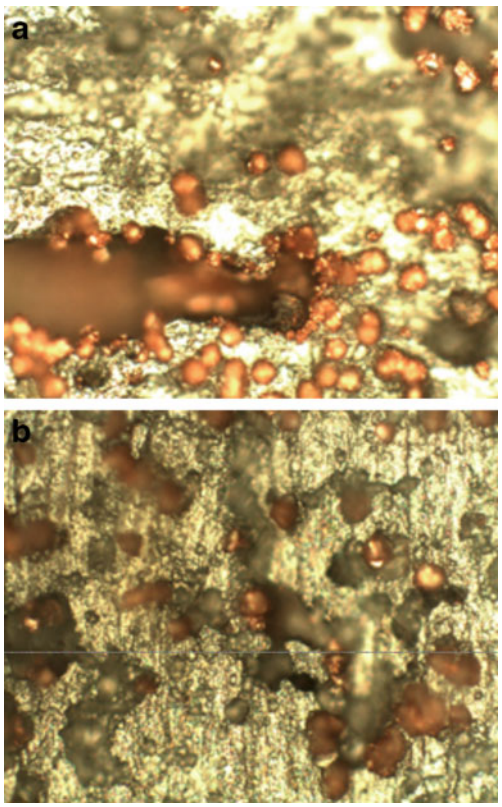

Fig. 10 Growth patterns of copper on used industrial blanks after 60 s, samples F1 (**a**) and G2 (**b**). Image size 1.40×1.75 mm

Discussion

Copper deposition in electrorefining and electrowinning is done from a complex sulfuric acid and copper sulfate electrolyte at current density of about 300 A/m^2. The substrate

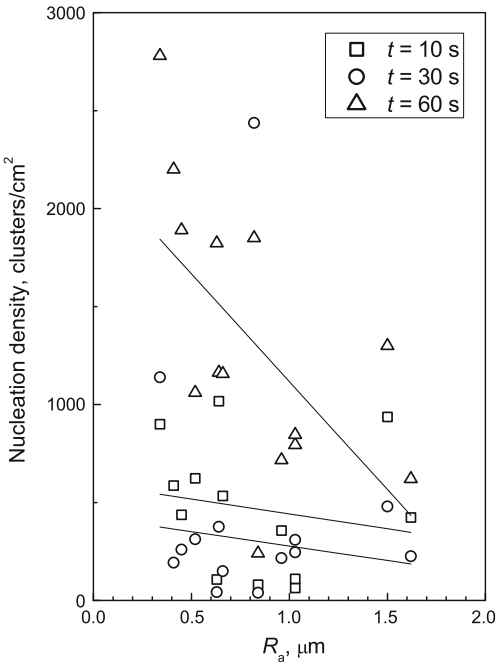

Fig. 11 Cluster density of tested industrial blank samples as function of surface roughness for t=10, 30, and 60 s

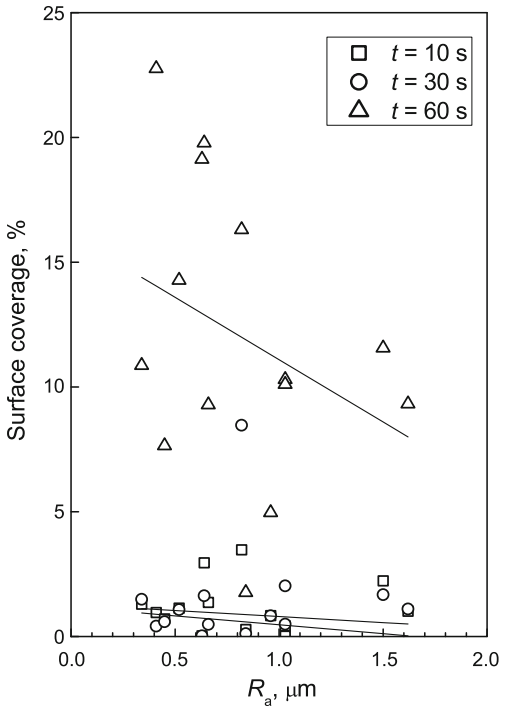

Fig. 12 Surface coverage of tested industrial blank samples as function of surface roughness for t=10, 30, and 60 s

for copper is often stainless steel that has been rolled to 2B surface finish and slightly etched to provide deeper grain boundaries for better adhesion. The 2B surface finish has roughness of R_a=0.1–0.5 μm and the typical grain size is 5 μm. During use, the surface will become worn and corroded causing higher surface roughness, scratches, and corrosion pits.

Copper deposition mechanisms have usually been studied using homogeneous substrates like platinum, glassy carbon, tungsten, titanium nitride, and silver. In this work, copper nucleation and growth were studied using stainless steel samples with original 2B surface finish and samples that had been water ground with 150 to 1200 grit emery paper. In addition, used industrial cathode blanks with irregular rough surfaces were used. The deposition tests were done with potentiostatic and galvanostatic methods using rotating disc electrodes, stationary electrodes, and Hull cell.

Both potentiostatic and galvanostatic RDE tests showed that copper deposits preferentially on the scratch marks. With roughest 150 grit sandpaper, copper deposited on both profile peaks and valleys, and on the smoother 800 grit and 1200 grit surfaces on profile peaks. On the RDE samples, cluster density was smaller but copper coverage increased faster when surface was smoother. Tests with stationary electrodes showed that on original 2B finish, copper deposition starts randomly from the grain boundaries and corners, where several grains contact. The grain boundaries and corners are energetically more active points than smooth grain faces, but all of these points are not equally active. When the surface was treated with emery paper, the effect of grain boundaries disappeared and deposition pattern followed the scratch lines.

Under galvanostatic conditions at the initial stages, nuclei are formed under non-stationary conditions and the overpotential changes with of time as more copper deposits on the surface. Galvanostatic polarization tests with clean samples showed continuous increase of potential (decrease in overpotential) with time. The potential change log|E| vs. log (t) was linear for nearly 10 s. As the deposition of copper on stainless steel requires high overpotential, the potential change can be explained by progressively easier deposition on existing copper. As copper coverage on the sample surface increases with time and average surface overpotential decreases, the most inactive parts of the stainless steel surface cannot support copper nucleation and growth due to too small local polarization. This can result in voids and electrolyte entrapment between stainless steel blank and copper cathode as often seen in copper electrorefining.

Copper deposition on tungsten using galvanostatic polarization has been found to follow a mechanism, where copper nucleation happens during the first seconds until a maximum overpotential has been reached and thereafter overpotential decreases as current is consumed in growth of existing copper crystals [21]. The maximum overpotential increases with increasing current density and the time to reach the maximum overpotential decreases with increasing current density. The current densities in this work were several orders of magnitude larger than in [21], and this explains why maximum overpotential was seldom noticed.

Deposition tests with industrial blanks showed two types of potential change with time: continuous decrease of overpotential or initial about 1-s increase of overpotential followed by decrease to a steady value. The deposition patterns on industrial blanks were not the same as the original 2B surface or water ground samples. The industrial blanks have much larger corrosion pits and other wear marks than the grain boundaries or scratch marks. Copper growth starts on the edges of larger damages and not on grain boundaries, plane surface, or shallow scratch marks. The cluster density was in the order of 10^3 nuclei/cm^2, also two or three orders of magnitude smaller than on 2B surface or water ground surface. The uneven start of copper deposition can explain lacy areas on cathode, thin cathodes, and impurities due to electrolyte entrapment sometimes seen in the tankhouses.

Conclusions

Copper deposition on stainless steel was studied using potentiostatic and galvanostatic deposition tests in synthetic copper electrorefining electrolyte. The SEM images from

RDE and Hull cell samples showed that on 2B stainless steel finish, copper nucleation and growth starts from grain boundaries and corners. When the surface has scratch marks, they act as preferential nucleation sites. Rough scratch marks support nucleation and growth on ridges and valleys whereas smooth marks on ridges only.

Optical images from deposition tests on stationary stainless steel samples showed that copper growth follows the scratch marks also for longer deposition times, up to 300 s. The growth of copper is initially more rapid at rough surfaces.

Deposition tests with old used industrial cathode blanks did not show clear patterns. These samples had in addition to scratch marks varying numbers of corrosion pits and deposits collected over the years. The number of copper clusters or area of copper decreased with increasing surface roughness. These results indicate that on rough surfaces the deposition is dominated by local current distribution.

Acknowledgments This work was financially supported by the International Copper Sponsor Group. The authors are grateful to the Group members for permission to publish the results.

References

1. Winand R (1998) Contribution to the study of copper electrocrystallization in view of industrial applications—submicroscopic and macroscopic considerations. Electrochim Acta 43(19–20):2925–2932
2. Plieth W (2010) The process chain of electrodeposition. Russ J Electrochem 46(10):1119–1124
3. Plieth W (2011) Electrocrystallization—factors influencing structure. J Solid State Electrochem 15:1417–1423
4. Budevski E, Staikov G, Lorenz WJ (1996) Electrochemical phase formation and growth. VCH, Weinheim
5. Zapryanova T, Jordanov N, Milchev A (2008) Electrochemical growth of single copper crystals on glassy carbon and tungsten substrates. J Electroanal Chem 612:47–52
6. Chang H, Choe B-H, Lee J (2005) Influence of titanium oxide films on copper nucleation during electrodeposition. Mater Sci Eng, A 409:317–328
7. Heerman L, Tarallo A (1999) Theory of the chronoamperometric transient for electrochemical nucleation with diffusion-controlled growth. J Electroanal Chem 470:70–76
8. Prentice G, Chen K (1998) Effects of current density on adhesion of copper electrodeposits to polyimide substrates. J Appl Electrochem 28(9):971–977
9. Vanden Brande P, Winand R (1993) First stages of the formation of copper electrodeposits and copper sputtered deposits on amorphous carbon and polycrystalline silver substrates. J Appl Electrochem 23:1089–1096
10. Grujicic D, Pesic B (2002) Electrodeposition of copper: the nucleation mechanisms. Electrochim Acta 47:2901–2912
11. Arzhanova T, Golikov A (2005) Spatial distribution of copper nuclei electrodeposited on glassy carbon under galvanostatic conditions. Corros Sci 47:723–734
12. Sun H, Delplancke J, Winand R, O'Keefe TJ (1991) Nucleation and growth of copper electrodeposits on titanium substrates. In: Copper–Cobre 91. pp 405–417
13. Kim S-B, Kim K-T, Park C-J, Kwon H-S (2002) Electrochemical nucleation and growth of copper on chromium-plated electrodes. J Appl Electrochem 32(11):1247–1255
14. Rao G, Cooper W (1979) The electrodeposition of copper on film-covered metal surfaces. Hydrometallurgy 4:185–207
15. Delplancke J-L, Sun M, O'Keefe T, Winand R (1990) Production of thin copper foils on microporous titanium oxide substrates. Hydrometallurgy 24:179–187
16. Zhou Z, O'Keefe T (1998) Electrodeposition of copper on thermally oxidized 316L stainless steel substrates. J Appl Electrochem 28:461–469
17. Urda-Kiel M, Oniciu L, Delplancke J-L, Winand R (1999) Nucleation and initial stages of copper electrodeposition on anodized 304 stainless steel. In: Dutrizac J, Ji J, Ramachandran V (eds) Copper 99–Cobre 99, Phoenix, Arizona, TMS, pp 511–528
18. O'Keefe TJ, Hurst L (1978) The effect of antimony, chloride ion, and glue on copper electrorefining. J Appl Electrochem 8:109–119
19. Moats M, Davenport W, Robinson T, Karcas G, Demetrio S (2007) Electrolytic copper refining—2007 world tankhouse data. In: Houlachi G, Edwards G, Robinson T (eds) Cu 2007, Toronto, Canada. Met Soc, pp 195–241
20. Zapryanova T, Hrussanova A, Milchev A (2007) Nucleation and growth of copper on glassy carbon: studies in extended overpotential interval. J Electroanal Chem 600:311–317
21. Peykova M, Michailova E, Stoychev D, Milchev A (1995) Galvanostatic studies of the nucleation and growth kinetics of copper in the presence of surfactants. Electrochim Acta 40 (16):2595–2601